Hydrothermal synthesis of ruthenium nanoparticles with a metallic core and a ruthenium carbide shell for low temperature activation of CO_2 to methane

Jorge Cored[a], Andrea García-Ortiz[a], Sara Iborra[a], María J. Climent[a], Lichen Liu[a], Cheng-Hao Chuang[b,c], Ting-Shan Chan[d], Carlos Escudero[e], Patricia Concepción[a,*], Avelino Corma[a,*]

[a] *Instituto de Tecnología Química, Universitat Politècnica de València-Consejo Superior de Investigaciones Científicas (UPV-CSIC), Avenida de los Naranjos s/n, 46022 Valencia, Spain*

[b] *Department of Physics, Tamkang University, Tamsui 25137 New Taipei City, Taiwan*

[c] *Research Center for X-Ray Science, Tamkang University, Tamsui 25137, New Taipei City, Taiwan*

[d] *National Synchrotron Radiation Research Center, Hsinchu 30076, Taiwan*

[e] *ALBA Synchrotron Light Source, Carrer de la Llum 2-26, 08290 Cerdanyola del Vallès, Spain*

- **ABSTRACT**

Ruthenium nanoparticles with a core-shell structure formed by a core of metallic ruthenium and a shell of ruthenium carbide have been synthesized by a mild and easy hydrothermal treatment. The dual structure and composition of the nanoparticles have been determined by synchrotron XPS and NEXAFS analysis and TEM imaging. At increasing sample depth, metallic ruthenium species start to predominate, according to depth profile synchrotron XPS and XRD analysis. The herein ruthenium carbon catalyst is able to activate both CO_2 and H_2 showing exceptional high activity for CO_2 hydrogenation at low temperatures (160-200 °C) with 100% selectivity to methane, surpassing by far the most active Ru catalysts reported up to now. Based on catalytic studies and isotopic $^{13}CO/^{12}CO_2/H_2$ experiments, the active sites responsible for the unprecedented activity can be associated to those surface ruthenium carbide (RuC) species, enabling CO_2 activation and transformation to methane *via* direct CO_2 hydrogenation mechanism. The high activity and absence of CO in the gas effluent confers this catalyst interest for the Sabatier reaction, a reaction with renewed interest for storing surplus renewable energy in the form of methane.

Keywords Ruthenium carbide, CO_2 activation, low temperature Sabatier, NEXAFS, synchrotron XPS, methane, hydrothermal synthesis, isotopic experiments.

- **INTRODUCTION**

The CO_2 concentration in the atmosphere has been growing exponentially in the last decade exceeding the 400 ppm in 2016 and leading to important environmental damages as, for instance, the global warming and sea water acidification.[1] Therefore, the reduction of CO_2 emissions is strongly required. Among the processes reported for CO_2 capture and use, CO_2 methanation reaction (so called Sabatier reaction) has received renewed interest in the last years as a way to store surplus renewable energy in the form of CH_4, which is easily stored, transported and used in the actual industrial infrastructure.[2] CO_2 methanation is a simple reaction, favoured thermodynamically at low temperatures (CO_2+ $4H_2 \leftrightarrow CH_4 + 2H_2O$; ΔH = -252.9 $KJ \cdot mol^{-1}$), but limited kinetically because of the high CO_2 stability. The catalysts proposed in patents and in the literature for producing CH_4 from CO_2 are based on metals like Ni, Ru, Pd, Rh, mono or multimetallic, with or without promoters (Na, K, Cs, rare-earth elements…) on different supports (TiO_2, SiO_2, Al_2O_3, CeO_2, ZrO_2, CNT doped with N).[3-5] In all cases high temperatures (300-500 °C) are employed which results in large energy input, high operational costs for large-scale production and with negative impact on catalyst stability. Ru is a highly active metal for CO_2 methanation at lower temperature, however the highest space time yield to methane reported up to now does not exceed the 0.9 $\mu mol_{CH4} \cdot s^{-1} \cdot g_{cat}^{-1}$ at 165 °C and 2.6 $\mu mol_{CH4} \cdot s^{-1} \cdot g_{cat}^{-1}$ at 200 °C and atmospheric pressure, obtained at a 1.6 $mL \cdot g^{-1} \cdot s^{-1}$ gas feed rate on a Ru/TiO_2 catalyst, still too low for industrial application.[6,7] Therefore, a breakthrough in the CO_2 methanation reaction will require a highly active and selective catalyst able to operate under mild reaction conditions.

Transition metal carbides appear as appealing catalyst alternatives with interesting catalytic properties for many processes, such as isomerization of n-heptane,[8] steam reforming of methanol,[9] dry reforming of methane,[10] CO hydrogenation,[11-13] and CO_2 hydrogenation.[14-18] Molybdenum carbide (β-Mo_2C)[14] and metal supported carbides (Me/Mo_2C[17] Me = Ni, Co, Cu; or Me/TiC[16] Me = Cu, Ni, Au) have shown high activity for CO_2 hydrogenation (i.e. 6-8% CO_2 conversion at 200 °C, 20 bar and 2.5 $mL \cdot g^{-1} \cdot s^{-1}$ gas feed rate),[17] being 3-5 times higher than the corresponding metals supported on typical oxide supports. However the selectivity to the target product is relatively low (29% and 42% CH_4 at 200 °C on β-Mo_2C and Ni/Mo_2C respectively)[17] due to CO formation (39% and 37% respectively). The high activity has been ascribed to the intrinsic activity of metal carbides to bind and activate the CO_2 molecule through a net charge carbide transfer to the CO_2 molecule.[15,19] The reactivity, i.e. C-O bond cleavage of the CO_2 molecule, depends strongly on the carbon/metal ratio. Thus, CO_2 dissociation occurs spontaneously on a Mo-terminated β-Mo_2C surface, yielding CO and O, while on a carbon rich surface (i.e. δ-MoC) a HOCO intermediate is formed, resulting in different product selectivity.

In an early study, Moreno-Castilla *et al*,[20] reported the formation of ruthenium carbide (RuC) in a Ru activated carbon catalyst prepared by sublimating $Ru_3(CO)_{12}$ on a carbon support, followed by thermal decarbonylation in He at 150 °C. Based on CO and H_2 chemisorption data, they argued the formation of a Ru^{IV} active phase, which according to the authors has been assigned to RuC. This result has to be reviewed considering the low tendency of ruthenium to form carbide or solid solution with carbon, requiring usually high pressure (5 GPa) and temperatures (1700-2500 °C) for their synthesis.[21-24] Moreover, the reported yield to methane in the CO_2/H_2 reaction was not higher (~1.4-1.0 times) than that of a similar sample without carbide species, which make the assignation to RuC doubtful.

In the present work, we show that it is possible to synthesize a ruthenium carbide catalyst (labelled as Ru@C) by an easy and mild hydrothermal method instead of using the reported high temperature and pressure treatments. Most importantly, the as synthesized Ru@C catalyst shows unprecedented activity for the low temperature (160-200 °C) CO_2 hydrogenation reaction to CH_4. Methane yields up to 3.5 $\mu mol_{CH4} \cdot s^{-1} \cdot g_{cat}^{-1}$ at 160 °C and 13.8 $\mu mol_{CH4} \cdot s^{-1} \cdot g_{cat}^{-1}$ at 200 °C, atmospheric pressure and at 8.3 $mL \cdot g^{-1} \cdot s^{-1}$ feed rate have been achieved, surpassing by far the most active Ru catalysts reported up to now.[5,6,7,25-26] The catalyst shows good stability under the operational conditions with CH_4 selectivity above 99.9%. We will show that the formation of CH_4 is taken place by direct activation and hydrogenation of CO_2.

- **EXPERIMENTAL SECTION**

Synthesis of Ru@C-EDTA

Samples at different Ru contents were prepared using the same synthesis method but modifying the amount of the Ru precursor. In general the synthesis method can be described as X (X = 1.5, 3.1, 5.3 and 6.6) g $Ru(acac)_3$ (Aldrich), 1.77 g Na_2EDTA (Aldrich) and 0.39 g NaOH (Acros) dissolved in 8 mL of deionized water. Then 4 mL of methanol were added to the mixed aqueous solution under stirring at room temperature, resulting in a red suspension, which was transferred into a 35 mL Teflon-coated stainless steel autoclave followed by static hydrothermal processing at 200 °C for 24 h. After it, the autoclave was taken out of the oven and cooled down to room temperature for 3 h. The generated precipitate was filtered and washed with deionized water and acetone five times. The samples were labelled as Ru@C-EDTA-X, where X corresponds to the ruthenium loading, determined by ICP (Table S1).

Synthesis of Ru@C-Glucose

120 mg of glucose (Aldrich) dissolved in 7 mL of deionized water was stirred at room temperature for 0.5 h. Then 100 mg of RuO_2 (Aldrich, 99.9%, particle size 32 nm determined by XRD) were added and mixed under ultra-sonication (Branson 3510 operating at 40 Hz) for 0.5 h,

obtaining a black suspension. The so obtained suspension was transferred into a Teflon-coated stainless steel autoclave of 12.5 mL. The autoclave was introduced in an oven placed at 175 °C and kept for 18 h under static conditions. After it, the autoclave was taken out of the oven and cooled down to room temperature for 2 h. The content of the autoclave was then filtrated under vacuum conditions recovering a black solid. The solid was washed five times first with water and later with acetone. Finally, it was dried in an oven at 60 °C for 12 h. The loading of ruthenium in the sample was 24.3 wt %, according to ICP analysis.

Synthesis of Ru/C-WI

The sample was prepared by a wet impregnation method as follows: 396 mg of $Ru(acac)_3$ were dissolved in 20 mL toluene for 0.5 h. Then 900 mg of carbon (activated charcoal Norit®, Aldrich) were added and stirred for 15 h at room temperature. The final solution was evaporated under vacuum resulting in a black solid. The solid was reduced in 50 mL·min^{-1} H_2 at 250 °C for 3 h with a heating ramp of 10 °C·min^{-1}, followed by cooling down in N_2 to 25 °C. After this, it was oxidised in 50 mL·min^{-1} O_2 flow at 400 °C for 3 h. The loading of ruthenium in the sample was 3.0 wt %, according to ICP analysis. XRD is shown in Figure S5.

Synthesis of Ru/C-Ar800

58 mg of $Ru(acac)_3$ were dissolved in 20 mL of acetone and stirred at 50 °C. 1.47 g of Na_2EDTA and 0.12 g NaOH were dissolved in water (20 mL) and the resulting aqueous solution was added to the metal solution and stirred for 0.5 h at 50 °C. Then, 1.6 g of carbon (activated charcoal Norit®) was added and the mixture was refluxed at 50 °C for 24 h. After cooling, the suspension was rotoevaporated, washed with water, filtered and dried at 100 °C overnight. The black solid was pyrolized in an Ar flow (10 mL·min^{-1}) at 800 °C for 5 h (5 °C·min^{-1}). XRD is shown in Fig. S5.

Synthesis of Ru@C/NG

The catalyst was synthesized according to Reference 27. Briefly, graphene oxide (GO) support was prepared following the improved Hummers method. GO was doped with nitrogen using formaldehyde (37% in water, Aldrich) and melamine (Acros) and the suspension was transferred into a Teflon-coated stainless steel autoclave (12.5 mL) and kept at 180 °C for 12 h. The gel obtained was submitted to pyrolysis in a N_2 flow at 750 °C for 5 h. NG support was dispersed in a phosphate buffered solution with the metal precursor ($RuCl_3 \cdot 3H_2O$, Johnson Matthey), dopamine hydrochloride (Aldrich) and CTAB (Acros) and hydrothermally treated at 140 °C for 6 h. The resulting suspension was centrifuged and the solid was washed with water and dried. The catalyst was obtained after a high temperature treatment in argon (800 °C, 10 mL·min^{-1}) for 3 h.

Ruthenium references

Commercial Ru on carbon, **Ru/C-com** (Acros Organics, 5 wt % Ru) and **Ru-Black** (Aldrich, >98%) were used as reference samples in catalytic and spectroscopic studies. XRD are shown in Figure S5.

Catalysts characterization

The Ru content was analysed by Inductively Coupled Plasma Optical Emission Spectrometry (ICP-OES) using a Varian 715-ES spectrometer. The samples were dissolved in aqua regia at 60 °C for 20 h. X-Ray powder diffraction (XRD) was recorded with a Philips X´Pert diffractometer using a monochromatic Cu Kα radiation (λ=0.15406 nm). Average particle size was calculated from the main peaks (38.4, 42.2, 44.0, 58.3, 69.4, 78.4; 2θ) of Ru^0 (JCPDS: 00-006-0663) using the Scherrer equation and assuming a shape factor k=0.9. Transmission Electron Microscopy (TEM) measurements were performed in a JEOL-JEM 2100F operating at 200 kV. Samples were prepared by dropping the suspension of the powder catalyst using ethanol as the solvent directly onto holey-carbon coated Cu grids. The amount of surface ruthenium metal sites was measured by CO chemisorption at 25 °C in a Quantachrome Autosorb-1C instrument by extrapolating the total gas uptakes in the adsorption isotherms at zero pressure and assuming an adsorption stoichiometry of 1:1 (Ru:CO).[20] Before measurements, about 300 mg of catalyst were activated in a helium flow at 100 °C (2 h) and in vacuum at the same temperature (1 h). Near Edge X-ray Absorption Fine Structure (NEXAFS) spectra at Ru L_3/L_2 edge were collected by the total fluorescence yield *via* Lytle detector at beamline 16A1 at Taiwan Light Source. The spot size was 0.5 x 0.5 (HxV) mm^2, where probed at the Ru powder sample by incident 45° angle. X-ray energy from Si (111) monocromator was calibrated using the energy jump of standard Mo foil at L_3 edge. Synchrotron X-ray Photoelectron Spectroscopy (XPS) experiments were performed at beamline BL24-CIRCE (NAPP branch) at ALBA Synchrotron Light Source (Cerdanyola del Vallès, Barcelona). At the NAPP branch from CIRCE, an undulator beamline with a photon energy range of 100-2000 eV, data acquisition was performed using a PHOIBOS 150NAP electron energy analyser (SPECS GmbH). The spectra were acquired with 20 µm exit slit and pass energy of 20 eV, and the X-ray spot was estimated to be in the order of 100 µm x 65 µm (HxV). Incident photon energies of 500 and 1150 eV for Ru 3d and C 1s were used to record the XPS spectra. Binding energies (BE) were calibrated with respect to C 1s signal settled at 284.5 eV. The sample (50 mg) was pelletized, mounted onto the sample holder and measured at room temperature at a 10^{-9} mbar pressure without previous activation. Shirley type background and Lorentzian type curves have been used in the spectra fitting. Laboratory X-ray Photoelectron Spectroscopy (XPS) experiments were performed on a SPECS equipment with a Phoibos 150 MCD-9 detector and using non- monochromatic AlKα (1486.6 eV) X-ray radiation. The pass energy was 20 eV and

the X-ray power 100 W. Raman studies were performed using a Renishaw "In via" spectrometer connected to an Olympia Microscope, and equipped with a He-Ne green laser (514 nm) and a diode laser (785 nm), and a CCD detector. Temperature Programmed Reduction with H_2 studies (TPR-H_2) were performed using a quartz reactor, connected online to a mass spectrometer Balzer (QMG 220M1). 120 mg of catalyst was used, flushed with Argon at 25 °C for 30 min, and switched to a 70% H_2 in Ar flow (14 mL·min^{-1}) and increasing the temperatures at 10 °C·min^{-1} to 160 , 180, 200, 220, 260 and 280 °C. The *m/z* values used for each product were 44 (CO_2), 28 (CO and CO_2), 2 (H_2), 15 (CH_4), 16 (CH_4) and 18 (H_2O).

Isotopic $^{13}CO/^{12}CO_2/H_2$ experiments

Catalytic tests with carbon labelled species were performed in a home-made stainless steel cell connected online with a mass spectrometer (Balzer QMG 220M1). The catalysts (15 mg) were pelletized and kept in vacuum at 120 °C for 0.5 h. In case of Ru/C-com, the sample was additionally reduced *in situ* with a H_2 flow (280 °C, 1 h, 10 mL·min^{-1}) before reaction. After activation, a mixture of $^{13}CO/^{12}CO_2/H_2$ (1:1:6 vol %) was fed continuously at 15 mbar total pressure. Then, the temperature was increased at 160 °C and finally the pressure was set at 25 mbar. The reaction evolution was monitored by Mass Spectrometry (MS) with *m/z* values: 44 ($^{12}CO_2$), 45 ($^{13}CO_2$), 28 (^{12}CO), 29 (^{13}CO), 15 ($^{12}CH_4$), 17 ($^{13}CH_4$), 18 (H_2O) and 2 (H_2).

CO_2 hydrogenation catalysis

CO_2 hydrogenation was performed in a stainless steel fixed bed reactor with an inner diameter of 11 mm and 240 mm length. Typically, 210 mg of catalyst (particle size 400-600 μm) were diluted in SiC in a weight ratio 0.14 (Cat/SiC). Ru@C-EDTA and Ru@C-glucose were not activated before reaction, while the other samples were *in situ* reduced prior to catalytic tests (25 mL·min^{-1} H_2, 280 °C, 1 h, 10 °C·min^{-1}). The reaction took place at atmospheric pressure and the reaction temperatures were 160, 180 and 200 °C. Each temperature was maintained for at least 1.5 h. The reaction was carried out at 21428 h^{-1} GHSV under concentrated (23.8 vol % CO_2, 71.3 vol % H_2, 5 vol % N_2) or diluted (5 vol % CO_2, 20 vol % H_2, 75 % vol N_2) conditions. Direct analysis of the reaction products was done by online gas chromatography (GC), using a SCION-456-GC equipment with TCD (MS-13X column) and FID (BR-Q Plot column) detectors. Blank experiments (in the presence of SiC) shown absence of homogeneous contribution to the reaction. Turnover frequency values (TOFs) were obtained from CO chemisorption data.

CO hydrogenation catalysis

CO hydrogenation was performed in the same reactor than CO_2 hydrogenation reaction. The inlet gas mixture was 30 % vol CO, 60 % vol H_2 and 10 % vol Ar with identical total flow (100 mL·min^{-1}). The process took place at atmospheric pressure and in a temperature range of 160-240 °C, using 210 mg of catalyst.

- **RESULTS AND DISCUSSION**

The Ru@C-EDTA samples are prepared under hydrothermal conditions (details in Experimental Section), modifying the amount of Ruthenium(III) acetylacetonate ($Ru(acac)_3$) in the synthesis gel, while keeping constant the ethylenediamine tetraacetic acid disodium salt (Na_2EDTA). The synthesis takes place at autogenous pressure at 200 °C for 24 h. The ruthenium loading in the as prepared samples, determined from ICP analysis, takes values between 28 wt % and 6 wt % (Table S1). Representative TEM images obtained from the Ru@EDTA samples are presented in Figure 1 and Fig.S1-S4, showing the presence of Ru^0 NP embedded in a carbon matrix. An homogeneous distribution of small Ru NP with average particle sizes of 2-5 nm are observed in the Ru@EDTA-6, Ru@EDTA-12 and Ru@EDTA-20 samples respectively, while a more heterogeneous size distribution containing small Ru NP of 2-5 nm and big Ru particles can be seen in the Ru@EDTA-28 sample (Fig.S4).

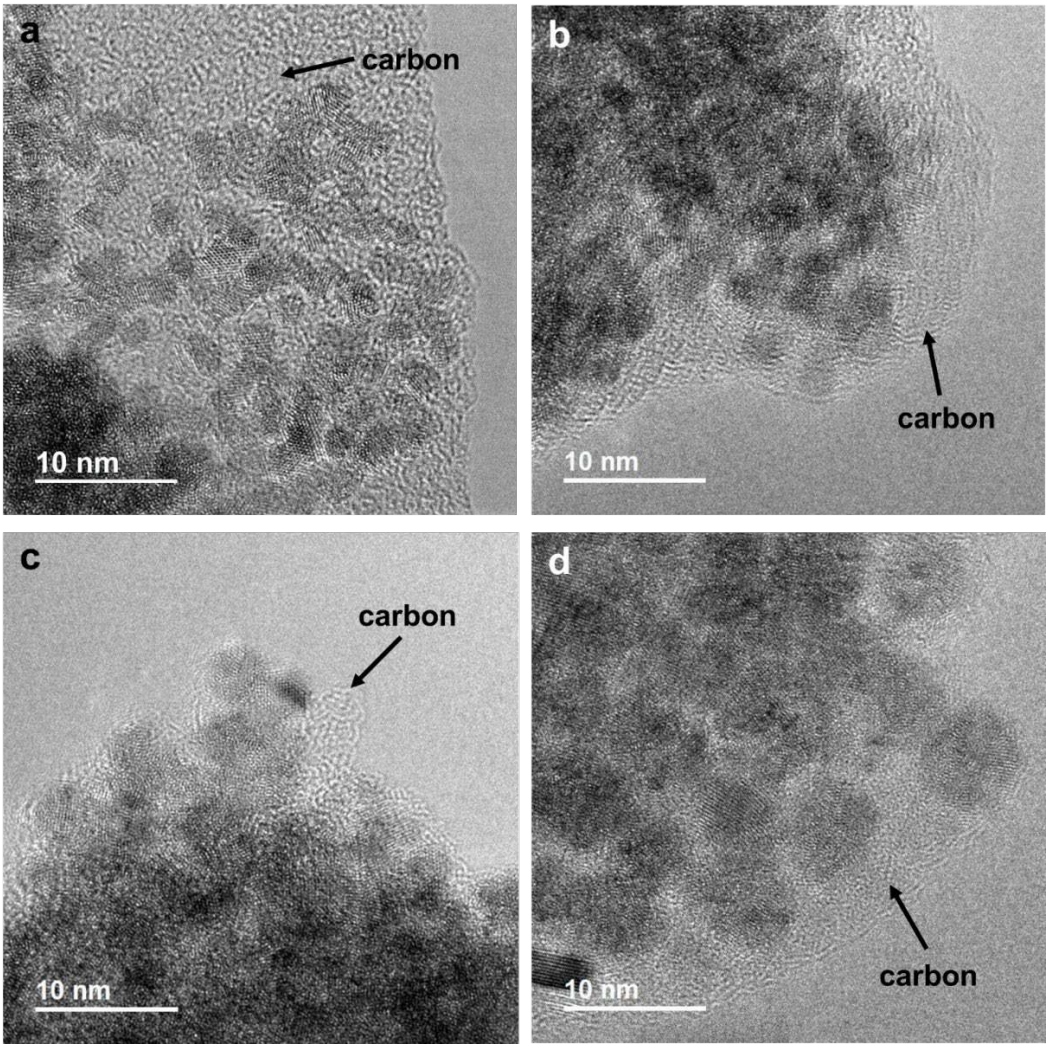

Figure 1. TEM images of various Ru@EDTA samples prepared with different ratios of Ru/EDTA by hydrothermal synthesis. (a) Ru@EDTA-6, (b) Ru@EDTA-12, (c) Ru@EDTA-20 and (d) Ru@EDTA-28.

This is in accordance with the X-ray diffractograms (Fig.S5) where the X-ray peak broadening observed in samples Ru@EDTA-6, Ru@EDTA-12 and Ru@EDTA-20 samples correspond with a small crystallite size, whereas some sharp peaks are visualized in the Ru@EDTA-28 sample corresponding to crystalline Ru^0 (hexagonal, JCPDS: 00-006-0663). The nature of the carbon matrix studied by Raman spectroscopy shows in all samples a graphitic structure (1600 cm^{-1}) with defects (1371 cm^{-1}) and some amorphous carbon (1506 cm^{-1})[29] (Fig.S6). XPS studies performed in a laboratory scale spectrometer using AlKα (1486.6 eV) X-ray energy (Fig.S7) show the presence of Ru^0 (279.3 eV) and RuO_2 (281.0 eV). However, when using surface sensitive high-resolution XPS spectroscopy using synchrotron radiation working at low X-ray excitation energy (500 eV) with a probing depth of around 2.2 nm,[30] the presence of an additional ruthenium specie at 279.6 eV than the Ru^0 (at 279.1 eV) and RuO_2 (281.0-280.4 eV) is clearly observed (Fig.2a). The surface concentration of this new specie increase slightly from ~56% to ~70% at decreasing the Ru content in the samples (Fig.2b).

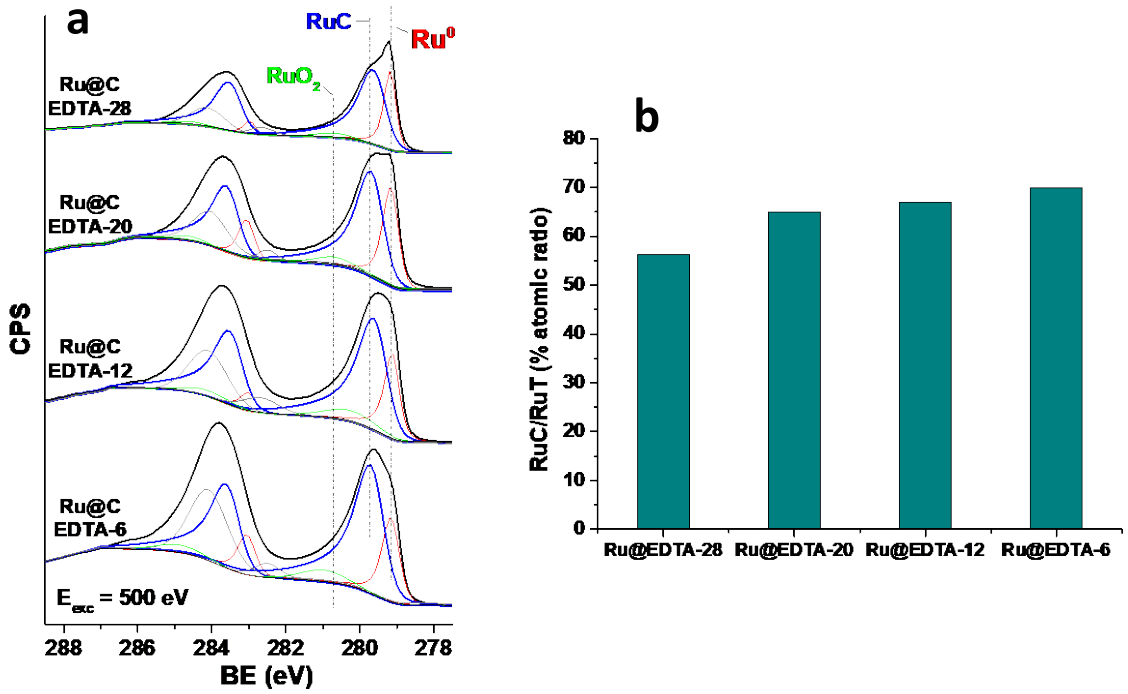

Figure 2. a) Synchrotron XPS of the C 1s and Ru $3d_{5/2}$ core level at 500 eV X-ray excitation energy on the fresh Ru@C-EDTA samples. Colour code for components: Ru^0 (red), RuC (blue) RuO_2 (green), C (grey). b) Surface concentration of the RuC phase relative to the total Ru (RuT).

Based on XPS depth profile analysis at a sample depth of 4.4 nm, the contribution of the new component at 279.6 eV to the total Ru peak intensity, decrease ~ 30-40 % in all samples at expense of the component of Ru^0 (Fig.S8), meaning that the new Ru specie identified by XPS is preferentially located on the upper surface layers of the catalyst. This new component has been ascribed in our work to ruthenium carbide (RuC) species. However, their assignation is not straightforward, due to the lack of reference data associated to RuC and uncertainties existing in the literature regarding the assignation of ruthenium chemical states.[31] Our assignation has been based on previous studies where a +0.5 eV shift respect to the metal has been related to carbide species,[32] and is also supported by HRTEM analysis (Fig.3a and Fig.S9), in where lattice fringes at 0.21 and 0.31 nm corresponding to Ru^0 and RuO_x respectively, and 0.28 nm due to RuC (PDF number 01-089-3016) are detected. In addition to XPS and HRTEM analysis, the assignation of the new detected specie to RuC has been supported by Near-Edge X-ray Absorption Fine Structure (NEXAFS) at the Ru $L_{2,3}$-edge performed on the Ru@C-EDTA-20 sample, and compared with RuO_2 or Ru^0 references (Fig.3b). The spectra reflect the electronic structure of surface Ru species and its local environment, which doesn't correspond to RuO_2 nor Ru^0. Indeed, the Ru $L_{2,3}$-edge white lines of Ru@C-EDTA-20 (located around 2840 and 2969 eV for the L_3 and L_2, respectively) are shifted to higher photon energy compared to that of Ru metal, and to lower energy respect to that of RuO_2, while are compatible with the RuC phase.[34] Moreover, the global spectral shapes characteristic of Ru^0 and RuO_2 result incompatible with the spectra collected on the Ru@C-EDTA-20 sample, where both the double peak structure around 2850 (L_3) / 2980 (L_2) eV (characteristic of the metal phase) and the one broadened peak structure of the white line (characteristic of the RuO_2 phase) are absent (details in Fig.S10(a),(b)). This agrees with the previous results and indicates that the upper surface of our catalyst is most likely ascribed to RuC. To our knowledge, this is the first time that a ruthenium carbide phase is formed under mild conditions (hydrothermal synthesis at 200 °C) in opposite to the harsh conditions (5 GPa and 1000-2500 °C) usually required for its synthesis.[21-24]

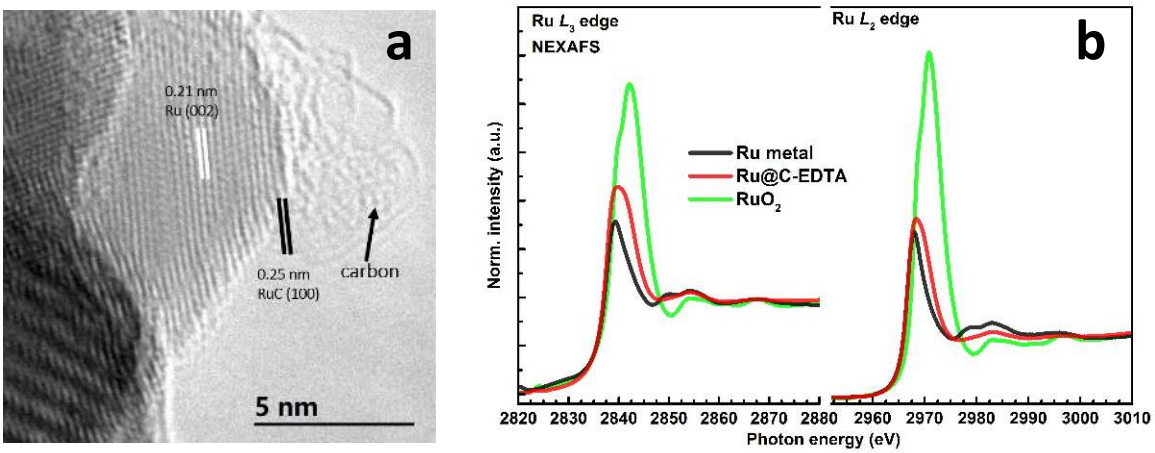

Figure 3. (a) HRTEM image of the Ru@C-EDTA-20 sample. (b) L_3-edge spectra (left panel) and L_2-edge spectra (right panel) of Ru^0, Ru@C-EDTA-20, and RuO_2.

From the point of view of their application in the CO_2 hydrogenation reaction, the thermal stability of the Ru@C-EDTA catalyst under H_2 rich conditions is proven by TPR-H_2 study (H_2 flow and atmospheric pressure), where the CH_4 formation (due to carbide and/or carbon hydrogenation) is followed by online Mass Spectrometry (MS). Under these conditions, CH_4 (*m/z*=15) clearly evolves at a temperature above 240 °C (Fig.S11), limiting the maximum temperature for catalytic studies to 240 °C.

The herein reported Ru@C-EDTA catalysts show markedly high activity at low temperature (160-200 °C) and atmospheric pressure for the CO_2 hydrogenation reaction, with 99.9% selectivity to methane, operating at 21428 h^{-1} GHSV (details in Experimental Section). The CO_2 conversion and the methane space time yield (STY_{CH4}) in the 160-180 °C temperature range at concentrated reaction conditions is summarized in Table 1, where an increase in the catalytic activity is observed at increasing Ru loading in the samples. The catalyst stability tested over a period of ~15 h reaction time at 160 °C on the Ru@C-EDTA-20 sample is plotted in Figure 4. A decrease in activity (~8%) is observed in the first 12 h of reaction, while it remains stable in the last 3 h. The observed loss of activity corresponds to a partial removal of surface ruthenium carbide species under reaction conditions, as evidenced from XPS studies using synchrotron radiation performed on the spent catalysts (Fig.S12a). In fact, a loss of RuC species is observed in all samples according to the XPS spectra acquired at 500 eV X-ray excitation energy, being in the order of 31-23% on the Ru@EDTA-6, Ru@EDTA-12, Ru@EDTA-20 samples and of 5% on the Ru@EDTA-28 sample (Fig.S12b). Based on this data, when plotting the amount of surface RuC of the spent Ru@C-EDTA catalysts with the STY_{CH4} at 160 °C of table 1a, a fairly good correlation

is found as displayed in Figure 5. These results suggest that the RuC species should play a key role in the catalytic activity of the Ru@C-EDTA samples, as discussed later.

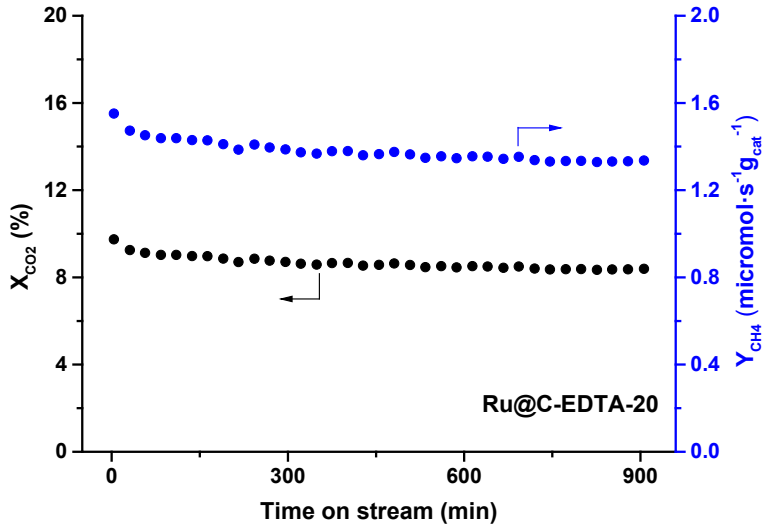

Figure 4. CO_2 conversion (left axe, black) and methane STY (right axe, blue) on the Ru@C-EDTA-20 catalyst at 160 °C, 21428 h^{-1} GHSV and 5% CO_2, 20% H_2 and 75% N_2 (% vol).

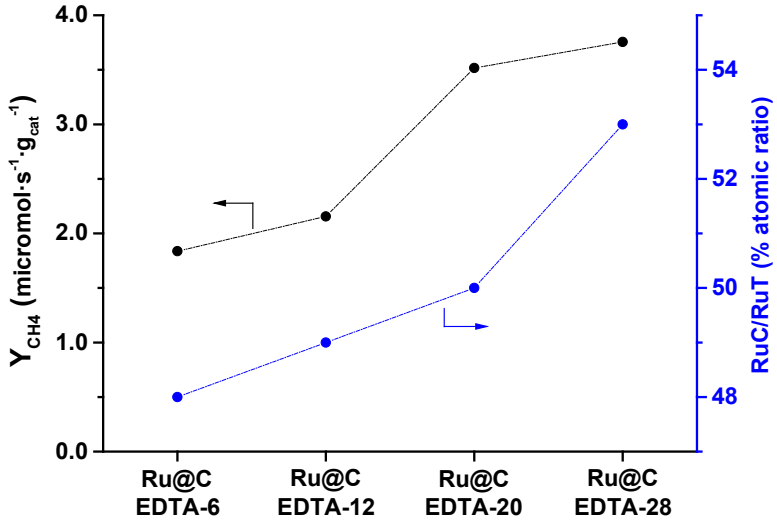

Figure 5. Methane STY (left axe, black) at 160 °C, 21428 h^{-1} GHSV and 23.8% CO_2, 71.3% H_2, 5% N_2 (% vol). On the right axe (blue), RuC/RuT atomic ratio obtained from XPS analysis on the spent Ru@C-EDTA catalysts at 500 eV X-ray excitation energy (Fig.S12).

The activity of the Ru@C-EDTA samples surpasses by far that of other synthesized ruthenium carbon catalysts as shown in Table 1b, and is markedly higher than that of most active ruthenium catalysts we found in the literature (Table S2). Being aware that the CO_2 methanation on Ru

catalysts has been reported to be size dependent, where large particles were found to be more active than smaller ones,[35] reference catalysts displaying different particle sizes have been considered. All catalysts prepared by different synthesis strategies, some of them reproducing those of the literature,[20,27,36] and the commercial type catalysts (such as Ru/C and Ru-Black) show negligible activity at the mild operation conditions considered here. Moreover, the selectivity to methane is almost 100 % on the Ru@C-EDTA samples, while other by-products like CO, C_xH_y are formed on the other samples (Fig.S13). Altogether endows in a very promising catalyst for the Sabatier reaction. In addition, the synthesis of this type of catalyst can be also achieved starting from other precursors like RuO_2 and glucose and using water as solvent (see Experimental Section and Fig.S14). The similar catalytic activity achieved in the Ru@C-Glucose catalyst, (see Table S3) allows to discard the enhanced catalytic activity of the Ru@C-EDTA catalysts to the presence of nitrogen or Na^+ additives coming from the Na_2EDTA precursor.

Taking into consideration that the reference ruthenium carbon catalysts of Table 1b have the ruthenium as Ru^0, while in Ru@C-EDTA catalysts the ruthenium at the surface is mainly RuC with some Ru^0, the much superior activity of the Ru@C-EDTA samples could be associated to the presence of RuC or to the combination of the two ruthenium phases, Ru^0 and RuC, and the carbon coating. In fact, if the RuC phase in Ru@C-EDTA is removed by treating the catalyst in H_2 at 280 °C, the catalytic activity strongly decreases (Fig.S15). This result reinforces our previous assumption of RuC species as a key component responsible of the high catalyst activity obtained in the CO_2 methanation reaction at low temperature.

Table 1. a) Catalytic activity in the CO_2 hydrogenation reaction at concentrated reaction conditions[a] on the Ru@C-EDTA samples; b) Catalytic activity at 160 °C of the Ru@C-EDTA-20 sample compared to other reference ruthenium carbon samples.

a)

Sample	160 °C		180 °C	
	X_{CO2} (%)	STY_{CH4} ($\mu mol_{CH4} \cdot s^{-1} \cdot g_{cat}^{-1}$)	X_{CO2} (%)	STY_{CH4} ($\mu mol_{CH4} \cdot s^{-1} \cdot g_{cat}^{-1}$)
Ru@EDTA-28	4.9	3.76	13.2	10.07
Ru@EDTA-20	4.6	3.52	9.8	7.56
Ru@EDTA-12	2.7	2.16	6.5	5.26
Ru@EDTA-6	1.3	1.84	2.5	3.48

b)

Sample	wt% Ru (Part. size)[f]	X_{CO2}[a] (%)	STY_{CH4} ($\mu mol_{CH4} \cdot s^{-1} \cdot g_{cat}^{-1}$)	(%) Selectivity CH_4 / CO / C_2H_6
Ru@C-EDTA-20	20.2% (--)	4.6	3.52	99.9 / 0 / 0.1
Ru/C-WI[b]	3.0% (17 nm)	<0.1	0.04	38.3 / 61.5 / 0.2
Ru/C-com	5.0% (2 nm)[g]	<0.1	0.07	92.7 / 6.8 / 0.5
Ru/C-Ar800[c]	4.0% -	0.1	<0.01	73.4 / 25.6 / 1.0
Ru@C/NG[d]	13.0%[27] -	0	-	-
$Ru_3(CO)_{12}$/C[e]	2.5% (1.2 nm)[20]	<0.1	0	0 / 100 / 0
Ru-Black Aldrich	100% (20 nm)	0.3	0.23	99.9 / 0 / 0.1

[a]1 bar, GHSV 21428 h^{-1}, reactant feed composed of 23.8 vol % CO_2, 71.2 vol % H_2, 5 vol % N_2; [b]Prepared by wet impregnation of $Ru(acac)_3$ on a carbon support; [c]Prepared by pyrolisis of the metal precursors according to ref. 36; [d]Prepared through thermal annealing of polydopamine (PDA) coated Ru NP supported on a three-dimensional N-doped graphene layer as in ref. 27; [e]Prepared from $Ru_3(CO)_{12}$ precursor as described in ref. 20; [f]Calculated by XRD; [g]Calculated by HRTEM.

The reaction mechanism (direct CO_2 hydrogenation or *via* reverse water gas-shift (RWGS)) of the Ru@C-EDTA samples have been studied combining catalytic studies using a CO/H_2 feed, with isotopic studies using a $^{13}CO/^{12}CO_2/H_2$ (1:1:6) reactant feed. For this purpose, the Ru@C-EDTA-20 catalyst has been used as reference sample of surface RuC species and its behaviour compared to a sample containing only Ru^0 (i.e. commercial Ru/C). Catalytic studies show negligible CO conversion (~0.01-0.05%) on the Ru@C-EDTA-20 sample in the 180-240 °C temperature range, while CO reacts in the commercial Ru/C sample (Table S4). Isotopic studies in the presence of both $^{13}CO/^{12}CO_2$ show a very high preferential $^{12}CO_2$ hydrogenation versus ^{13}CO on the Ru@C-EDTA-20 sample, since only $^{12}CH_4$ is detected (Fig.S16a). Meanwhile on the Ru/C sample ^{13}CO is preferentially hydrogenated versus $^{12}CO_2$, resulting in $^{13}CH_4$ formation

(Fig.S16b). Combining both results and taken into account the selectivity obtained during the CO_2 hydrogenation, in where CO was not detected in the Ru@C-EDTA-20 sample, while it is formed as by-product in the Ru/C sample (Fig.S13), we can conclude that a direct CO_2 hydrogenation path to CH_4 takes place on the Ru@C-EDTA-20 sample, while contribution of a RWGS reaction mechanism occurs on the Ru/C sample in the presence of Ru^0, in agreement to previous studies. [35,37-42] Moreover, the fact that $^{13}CH_4$ is not observed in the isotopic studies of the Ru@C-EDTA-20 sample allows to discard the co-existence of Ru^0 species on the catalyst surface or, if present, it should be in a very low amount, being the activity ascribed predominately to the presence of RuC species. Based on it, a core shell structure containing a metallic core and an upper shell of ruthenium carbide and carbon species can be proposed in our catalysts. The RuC phase has been proven to be the active specie in the CO_2 hydrogenation, which in accordance with the literature[15,19] favour CO_2 binding and activation.

CONCLUSION

In conclusion, we have described an easy synthesis method allowing the stabilization of surface ruthenium carbide species, while ruthenium metal predominate at increasing sample depths. Those RuC surface species enables CO_2 activation, which is hydrogenated to methane in a direct reaction path, yielding 100% selectivity to CH_4. The high activity at low temperature (160-200 °C) and absence of CO in the gas effluent makes the herein synthesized Ru@C-EDTA and Ru@C-Glucose samples very promising candidates for the Sabatier reaction.

▪ ASSOCIATED CONTENT

Supporting Information includes XRD diffractograms of tested materials; Raman spectra of Ru@C-EDTA-20 sample; LAB XPS; C 1s and Ru 3d Synchrotron XPS core levels of the Ru@C-EDTA samples; HRTEM images of Ru@C-EDTA samples; NEXAFS experiments; TPR-H_2 profile of Ru@C-EDTA-20; Catalytic results on Sabatier reaction at atmospheric pressure of Ru@C-EDTA-20, RU@C-glucose and other reference samples; State of art in Sabatier reaction; Catalysis with Syngas; Isotopic $^{13}CO/^{12}CO_2$ experiments.

▪ AUTHOR INFORMATION

Corresponding authors

*pconcepc@upvnet.upv.es

*acorma@itq.upv.es

ORCID

Patricia Concepción 0000-0003-2058-3103

Avelino Corma 0000-0002-2232-3527

Author contributions

A.C. conceived the project, directed the study together with P.C. and contributed in the production of the manuscript. P.C. wrote the manuscript, did the Raman and $^{13}CO/^{12}CO_2/H_2$ isotopic experiments and participated together with C.E. in the XPS measurements at ALBA Synchrotron. J.C. did the catalytic study. A.G.O. did the synthesis of the samples. L.L. carried out the TEM measurements. C.H.C. and T.S.C. performed the NEXAFS analysis at Taiwan Light Source. S.I. and M.J.C. participated in the discussion of the results together with all other authors.

Notes

The authors declare no competing financial interest.

▪ ACKNOWLEDGMENTS

The research leading to these results has received funding from the Spanish Ministry of Science, Innovation and Universities through "Severo Ochoa" Excellence Programme (SEV-2016-0683) and the PGC2018-097277-B-100 (MCIU/AEI/FEDER, UE) project. The authors also thank the Microscopy Service of UPV for kind help on measurements. A. García-Ortiz thanks "Severo Ochoa" Programme (SEV-2016-0683) for a predoctoral fellowship. C. H. Chuang acknowledges financial support from MOST project 107-2112-M-032-005. J. Cored thanks the Spanish Government (MINECO) for a "Severo Ochoa" grant (BES-2015-075748). The authors thanks the support of ALBA Synchrotron Light Source staff for the successful performance of the measurements at CIRCE beamline (BL24).

▪ ABBREVIATIONS

CNT, carbon nanotube; acac, acetylacetonate; EDTA, ethylenediaminetetraacetic acid derived salt; CTAB, Cetyl Trimethyl Ammonium Bromide; wt, weight; vol, volume.

▪ REFERENCES

(1) Yuan, Z.; Eden, M. R.; Gani, R. Toward the Development and Deployment of Large-Scale Carbon Dioxide Capture and Conversion Processes. *Ind. Eng. Chem. Res.* **2016**, *55*, 3383-3419.

(2) Stangeland, K.; Kalai, D.; Li, H.; Yu, Z. CO_2 Methanation: The Effect of Catalysts and Reaction Conditions. *Energy Procedia* **2017**, *105*, 2022-2027.

(3) Solis-Garcia, A.; Fierro-Gonzalez, J. C. Mechanistic Insights into the CO_2 Methanation Catalyzed by Supported Metals: A review. *J. Nanosci. Nanotechnol.* **2019**, *19*, 3110-3123.

(4) Panagiotopoulou, P. Hydrogenation of CO_2 over supported noble metal catalysts. *Appl. Catal. A: Gen.* **2017**, *542*, 63-70.

(5) Qin, Z.; Zhou, Y.; Jiang, Y.; Liu, Z.; Ji, H. Recent advances in heterogeneous Catalytic Hydrogenation of CO_2 to methane: Chapter 4. In *New Advances in Hydrogenation Processes-Fundamentals and Applications*; http://dx.doi.org/10.5772/65407 Intechopen: 2017; pp 57-82.

(6) Kim, A.; Sanchez, C.; Patriarche, G.; Ersen, O.; Moldovan, S.; Wisnet, A.; Sassoye, C.; Debecker, D. P. Selective CO_2 methanation on Ru/TiO_2 catalysts: unravelling the decisive role of the TiO_2 support crystal structure. *Catal. Sci. Technol.* **2016**, *6*, 8117-8128.

(7) Lin, Q.; Liu, X. Y.; Jiang, Y.; Wang, Y.; Huang, Y.; Zhang, T. Crystal phase effects on the structure and performance of ruthenium nanoparticles for CO_2 hydrogenation. *Catal. Sci. Technol.* **2014**, *4*, 2058-2063.

(8) Lamic, A. F.; Pham, T. L. H.; Potvin, C.; Manoli, J. M.; Mariadassou, G. D. Kinetics of bifunctional isomerization over carbides (Mo, W). *J. Mol. Catal. A-Chem.* **2005**, *237*, 109-114.

(9) Ma, Y.; Guan, G.; Hao, X.; Zuo, Z.; Huang, W.; Phanthong, P.; Kusakabe, K.; Abudula, A. Highly-efficient steam reforming of methanol over copper modified molybdenum carbide. *RSC. Adv.* **2014**, *4*, 44175-44184.

(10) Shi, C.; Zhang, A.; Li, X.; Zhang, S.; Zhu, A.; Ma, Y.; Au, C. Ni-modified Mo_2C catalysts for methane dry reforming. *Appl. Catal. A: Gen.* **2012**, *431-432*, 164-170.

(11) Christensen, J. M.; Duchstein, L. D. L.; Wagner, J. B.; Jensen, P. A.; Temel, B.; Jensen, A. D. Catalytic Conversion of Syngas into Higher Alcohols over Carbide Catalysts. *Ind. Eng. Chem. Res.* **2012**, *51*, 4161-4172.

(12) Liu, C.; Lin, M.; Jiang, D.; Fang, K.; Sun, Y. Preparation of Promoted Molybdenum Carbides Nanowire for CO Hydrogenation. *Catal. Lett.* **2014**, *144*, 567-573.

(13) Yin, K.; Shou, H.; Ferrari, D.; Jones, C. W.; Davis, R. J. Influence of Cobalt on Rubidium-Promoted Alumina-Supported Molybdenum Carbide Catalysts for Higher Alcohol Synthesis from Syngas. *Top. Catal.* **2013**, *56*, 1740-1751.

(14) Xu, W.; Ramirez, P. J.; Stacchiola, D.; Rodriguez, J. A. Synthesis of α-MoC_{1-x} and β-MoC_y Catalysts for CO_2 Hydrogenation by Thermal Carburization of Mo-oxide in Hydrocarbon and Hydrogen Mixtures. *Catal. Lett.* **2014**, *144*, 1418-1424.

(15) Posada-Pérez, S.; Viñes, F.; Ramirez, P. J.; Vidal, A. B.; Rodriguez, J. A.; Illas, F. The bending machine: CO_2 activation and hydrogenation on δ-MoC(001) and β-Mo_2C(001) surfaces. *Phys. Chem. Chem. Phys.* **2014**, *16*, 14912-14921.

(16) Rodriguez, J. A.; Evans, J.; Feria, L.; Vidal, A. B.; Liu, P.; Nakamura, K.; Illas, F. CO_2 hydrogenation on Au/TiC, Cu/TiC, and Ni/TiC catalysts: Production of CO, methanol, and methane. *J. Catal.* **2013**, *307*, 162-169.

(17) Xu, W.; Ramírez, P. J.; Stacchiola, D.; Brito, J. L.; Rodriguez, J. A. The carburization of transition metal molybdates (M_xMoO_4, M=Cu, Ni or Co) and the generation of highly active metal/carbide catalysts for CO_2 hydrogenation. *Catal. Lett.* **2015**, *145*, 1365-1373.

(18) Liu, X.; Song, Y.; Geng, W.; Li, H.; Xiao, L.; Wu, W. Cu-Mo_2C/MCM-41: An Efficient Catalyst for the Selective Synthesis of Methanol from CO_2. *Catalysts* **2016**, *6*, 75.

(19) Nagai, M.; Oshikawa, K.; Kurakami, T.; Miyao, T.; Omi, S. Surface Properties of Carbided Molybdena-Alumina and Its Activity for CO_2 Hydrogenation *J. Catal.* **1998**, *180*, 14-23.

(20) Moreno-Castilla, C.; Salas-Peregrín, M. A.; López-Garzón, F. J. Hydrogenation of carbon oxides by Ru/activated carbon catalysts obtained from $Ru_3(CO)_{12}$: effect of pretreatment on their dispersion, composition and activity. *J. Mol. Catal. A: Chem.* **1995**, *95*, 223-233.

(21) Jiménez-Villacorta, F.; Álvarez-Fraga, L.; Bartolomé, J.; Climent-Pascual, E.; Salas-Colera, E.; Aguilar-Pujol, M. X.; Ramírez-Jiménez, R.; Cremades, A.; Prieto, C.; Andrés, A. Nanocrystalline cubic ruthenium carbide formation in the synthesis of graphene on ruthenium ultrathin films. *J. Mater. Chem. C.* **2017**, *5*, 10260-10269.

(22) Zhao, Z.; Meng, C.; Li, P.; Zhu, W.; Wang, Q.; Ma, Y.; Shen, G.; Bai, L.; He, H.; He, D.; Yu, D.; He, J.; Xu, B.; Tian, Y. Carbon coated face-centered cubic Ru-C nanoalloys. *Nanoscale* **2014**, *6*, 10370-10376.

(23) Sun, W.; Chakraborty, S.; Ahuja, R. Stabilizing a hexagonal Ru_2C via Lifshitz transition under pressure. *Appl. Phys. Lett.* **2013**, *103*, 251901.

(24) Sanjay Kumar, N. R.; Chandra Shekar, N. V.; Chandra, S.; Basu, J.; Divakar, R.; Sahu, P. C. Synthesis of novel Ru_2C under high pressure-high temperature conditions. *J. Phys.: Condens. Matter.* **2012**, *24*, 362202.

(25) Abe, T.; Tanizawa, M.; Watanabe, K.; Taguchi, A. CO_2 methanation property of Ru nanoparticle-loaded TiO_2 prepared by a polygonal barrel-sputtering method. *Energy Environ. Sci.* **2009**, *2*, 315-321.

(26) Li, D.; Ichikuni, N.; Shimazu, S.; Uematsu, T. Hydrogenation of CO_2 over sprayed Ru/TiO_2 fine particles and strong metal-support interaction. *Appl. Catal. A: Gen.* **1990**, *180*, 227-235.

(27) Li, Y.; Zhang, L. A.; Qin, Y.; Chu, F.; Kong, Y.; Tao, Y.; Li, Y.; Bu, Y.; Ding, D.; Liu, M. Crystallinity Dependence of Ruthenium Nanocatalyst toward Hydrogen Evolution Reaction. *ACS Catal.* **2018**, *8*, 5714-5720.

(28) Martínez Tejada, L. M.; Muñoz, A.; Centeno, M. A.; Odriozola, J. A. In-situ Raman spectroscopy study of Ru/TiO_2 catalyst in the selective methanation of CO. *J. Raman Spectrosc.* **2016**, *47*, 189-197.

(29) Sadezky, A.; Muckenhuber, H.; Grothe, H.; Niessner, R.; Pöschl, U. Raman microspectroscopy of soot and related carbonaceous materials: Spectral analysis and structural information. *Carbon* **2005**, *43*, 1731-1742.

(30) Tougaard, S. QUASES: Software packages to characterize surface nano-structures by analysis of electron spectra. http://www.quases.com/products/quases-imfp-tpp2m/

(31) Morgan, D. J. Resolving ruthenium: XPS studies of common ruthenium materials. *Surf. Interface Anal.* **2015**, *47*, 1072-1079.

(32) Teschner, D.; Borsodi, J.; Wootsch, A.; Révay, Z.; Hävecker, M.; Knop-Gericke, A.; Jackson S. D., Schlögl, R. The Roles of Subsurface Carbon and Hydrogen in Palladium-Catalyzed Alkyne Hydrogenation. *Science* **2008,** *320*, 86-89.

(33) Park, J.; Lee, J. W.; Ye, B. U.; Chun, S. H.; Joo, S. H.; Park, H.; Lee, H.; Jeong, H. Y.; Kim, M. H.; Baik, J. M. Structural Evolution of Chemically-Driven RuO_2 Nanowires and 3-Dimensional Design for Photo-Catalytic Applications. *Scientific Reports* **2015**, *5*, 11933.

(34) Liu, J.; Zhang, L. L.; Zhang, J.; Liu, T.; Zhao, X. S. Bimetallic ruthenium-copper nanoparticles embedded in mesoporous carbon as an effective hydrogenation catalyst Nanoscale **2013**, *5*, 11044-11050.

(35) Wang, X.; Hong, Y.; Shi, H.; Szanyi, J. Kinetic modeling and transient DRIFTS–MS studies of CO_2 methanation over Ru/Al_2O_3 catalysts. *J. Catal.* **2016**, *343*, 185-195.

(36) Hertrich, M. F.; Scharnagl, F. K.; Pews-Davtyan, A.; Kreyenschulte, C. R.; Lund, H.; Bartling, S.; Jackstell, R.; Beller, M. Supported Cobalt Nanoparticles for Hydroformylation Reactions. *Chem. Eur. J.* **2019**, *25*, 5534-5538.

(37) Marwood, M.; Doepper, R.; Renken, A. In-situ surface and gas phase analysis for kinetic studies under transient conditions: The catalytic hydrogenation of CO_2. *Appl. Catal. A: Gen.* **1997**, *151*, 223-246.

(38) Panagiotopoulou, P.; Kondarides, D. I.; Verykios, X. E. Mechanistic aspects of the selective methanation of CO over Ru/TiO_2 catalyst. *Catal. Today* **2012**, *181*, 138-147.

(39) Sachtler, J. W. A.; Kool, J. M.; Ponec, V. The role of carbon in methanation by cobalt and ruthenium. *J. Catal.* **1979**, *56*, 284-286.

(40) Panagiotopoulou, P.; Verykios, X. E. Mechanistic Study of the Selective Methanation of CO over Ru/TiO_2 Catalysts: Effect of Metal Crystallite Size on the Nature of Active Surface Species and Reaction Pathways. *J. Phys. Chem. C.* **2017**, *121*, 5058-5068.

(41) Zhao, K.; Wang, L.; Calizzi, M.; Moioli, E.; Züttel, A. In Situ Control of the Adsorption Species in CO_2 Hydrogenation: Determination of Intermediates and Byproducts. *J. Phys. Chem. C* **2018**, *122*, 20888-20893.

(42) Eckle, S.; Anfang, H. G.; Behm R. J.; Reaction Intermediates and Side Products in the Methanation of CO and CO_2 over Supported Ru Catalysts in H_2-Rich Reformate Gases. *J. Phys. Chem. C* **2011**, *115*, 1361-1367.

- **GRAPHICAL ABSTRACT (“For Table of Contents Only”)**